analytical chemistry

Article

pubs.acs.org/ac

Open Access on 01/10/2015

Development and Quantitative Evaluation of a High-Resolution Metabolomics Technology

Xiaojing Liu, Zheng Ser, and Jason W Locasale*

Division of Nutritional Sciences, Cornell University, Ithaca, New York 14853, United States

Supporting Information

ABSTRACT: Recent advances in mass spectrometry have allowed for unprecedented characterization of human metabolism and its contribution to disease. Despite these advances, limitations in metabolomics technology remain. Here, we describe a metabolomics strategy that consolidates several recent improvements in mass spectrometry technology. The platform involves a high-resolution Orbitrap mass spectrometer coupled to faster scanning speeds, allowing for polarity switching and improved ion optics resulting in enhanced sensitivity. When coupled to HILIC chromatography, we are able to quantify over 339 metabolites from an extract of HCT8 cells with a linear range of over 4 orders of magnitude in a single chromatographic run. These metabolites include diverse chemical classes ranging from amino acids to polar lipids. In addition, we also detect over 3000 additional potential metabolites present in mammalian cells. We applied this platform to characterize the metabolome of eight colorectal cancer cell lines and observed both commonalities and heterogeneities across their metabolic profiles when cells are grown in identical conditions. Together these results demonstrate that simultaneous profiling and quantitation of the human metabolome is feasible.

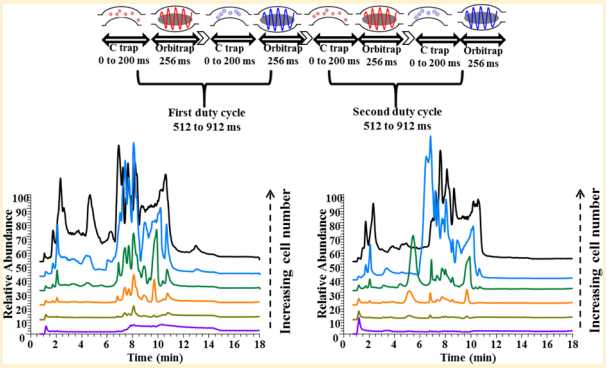

Advances in mass spectrometry have allowed for the simultaneous measurement and quantitation of many metabolites in defined biological conditions.[1−4] These advances in metabolomics have led to newfound insights into the role of metabolism in health and disease. For example, tumor cells are known to have dramatic alterations in the ability to uptake and metabolize nutrients, resulting in gross rewiring of the metabolic network.[5−10] Mass spectrometry has played an instrumental role in defining these differences that are now being investigated for cancer treatment and prevention.

These metabolomic technologies have involved high-performance liquid chromatography (HPLC) coupled to an electrospray ion (ESI) source and mass analyzer. Typically, the platforms have used a triple quadrupole mass analyzer and involve targeting a series of metabolites by monitoring the transitions from the selected precursor ion to a specific fragmentation ion of the precursor ion (multiple reaction monitoring, MRM).[11,12] Alternatively, instruments utilizing high-resolution mass spectrometry (HRMS) tend to have higher duty cycle times, leading to difficulties in quantitation.[13−15] An instrument that consolidates these capabilities could allow for untargeted metabolite profiling with sufficient scan speeds for quantitative, targeted analysis. Such an advance might overcome many of the limitations in both approaches. Scan speeds have also improved such that polarity switching is obtainable on these instruments, allowing for approximately a 2-fold expansion of the number of metabolites that can be detected during single chromatographic runs.[16−20]

In light of these advances, the extent of capability that this current metabolomics technology could allow remains poorly characterized. We developed a HRMS-based metabolomics platform using HPLC coupled to a heated ESI source (HESI), a quadrupole mass filter, a curved ion trap (C-trap), and Fourier transform-based OrbitrapTM mass analyzer. This instrument, termed the Q-Exactive MS (QE-MS), has demonstrated many superior capabilities for quantitative and qualitative proteomics applications,[21−24] but its general utility for metabolomics applications has, to our knowledge, yet to be explored. We next considered an extensive assessment of its performance in both targeted and nontargeted applications by evaluating its ability to detect and quantify metabolomics across a set of colorectal cancer cell lines.

EXPERIMENTAL SECTION

Materials. All cell lines were provided as a generous gift from Dr. Lewis Cantley's laboratory. RPMI 1640 medium was purchased from Cellgro. Fetal Bovine Serum (FBS), penicillin, and streptomycin were purchased from Hyclone Laboratories. Dialyzed FBS was obtained from Life Technologies. Optima-grade ammonium acetate, ammonium hydroxide, acetonitrile, methanol, and water were purchased from Fisher Scientific.

Received: November 26, 2013
Accepted: January 10, 2014
Published: January 10, 2014

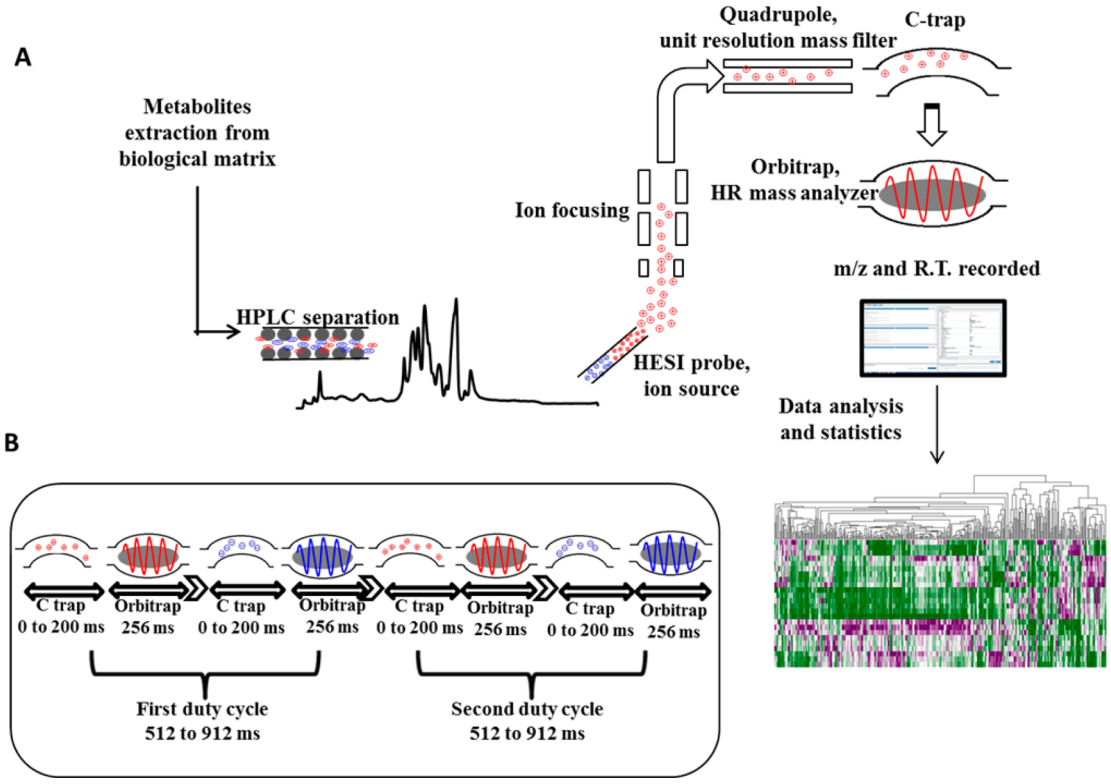

Figure 1. Overview of polar metabolite analysis platform. (A) The platform for polar metabolomics using LC-QE-MS. In positive mode, positively charged ions (red dots) are sent to S-lens (ion focusing), a quadrupole (low-resolution mass filter), C-trap (ions accumulate here until the targeted number of ions is reached), and finally Orbitrap high-resolution (HR) mass analyzer, where mass to charge ratio (m/z) of each ion and corresponding retention time (R.T.) are recorded. Once positive ions are sent to the Orbitrap from C-trap, the electronic field polarity is reversed, and only negatively charged ions (blue dots) are delivered from the HESI probe. (B) The duty cycle time when instrument is operated in pos/neg switch full scan mode with resolution of 70000. The typical duty cycle is between 512 and 912 ms, depending on the C-trap injection time (IT).

Cell Culture. All cell lines were first cultured in 10 cm dishes with full growth medium, which contains RPMI 1640, 10% FBS, 100 units/mL penicillin and 100 μg/mL streptomycin. Cells were grown in a 37 °C incubator with 5% CO_2.

Mass Spectrometry. The QE-MS is equipped with a HESI probe, and the relevant parameters are as listed: heater temperature, 120 °C; sheath gas, 30; auxiliary gas, 10; sweep gas, 3; spray voltage, 3.6 kV for the positive mode and 2.5 kV for the negative mode. Capillary temperature was set at 320 °C, and S-lens was 55. A full scan range from 60 to 900 (m/z) was used. The resolution was set at 70000. The maximum injection time (max IT) was 200 ms with typical injection times around 50 ms. These settings resulted in a duty cycle of around 550 ms to carry out scans in both the positive and negative modes. Automated gain control (AGC) was targeted at 3×10^6 ions. For MS/MS, the isolation width of the precursor was set at 2.5, HCD collision energy was 35%, and max IT is 100 ms. The resolution and AGC were 35000 and 200000, respectively. Full scan with resolution at 35000 and IT of 100 ms) was run together with MS/MS. Customized mass calibration was performed before any sample analysis.

High-Performance Liquid Chromatography. The HPLC (Ultimate 3000 UHPLC) is coupled to QE-MS (Thermo Scientific) for metabolite separation and detection. An Xbridge amide column (100 × 2.1 mm i.d., 3.5 μm; Waters) is employed for compound separation at room temperature. The mobile phase A is 20 mM ammonium acetate and 15 mM ammonium hydroxide in water with 3% acetonitrile, pH 9.0, and mobile phase B is acetonitrile. The linear gradient used is as follows: 0 min, 85% B; 1.5 min, 85% B, 5.5 min, 35% B; 10 min, 35% B, 10.5 min, 35% B, 14.5 min, 35% B, 15 min, 85% B, and 20 min, 85% B. The flow rate was 0.15 mL/min from 0 to 10 min and 15 to 20 min and 0.3 mL/min from 10.5 to 14.5 min.

Sample Preparation for Dynamic Range Studies. HCT 8 cells were grown in three 10 cm dishes with full growth medium. When the cells reach 80% confluence, the media were quickly removed, and the dish was placed on top of dry ice. Three milliliters of extraction solvent was immediately added (80% methanol/water), and the dishes were then transferred to the −80 °C freezer. The dishes were left for 15 min, and then cells were scraped into extraction solvent on dry ice. The entirety of the solution was transferred to two 1.7 mL eppendorf tubes and centrifuged with the speed of 20000g for 10 min at 4 °C. Here, cell metabolite extracts were prepared from three separate dishes to make three biological replicates. The supernatant was then transferred to new eppendorf tubes and dried in a SpeedVac. The samples can also be dried under nitrogen gas. After drying, one tube of each sample was stored in the −80 °C freezer as a backup, while the other one was reconstituted into 20 μL of water (LC−MS grade, Fisher Scientific). A serial dilution of triplicate samples from 10 cm Petri dish was done 5 times with a dilution factor of 6, ending up with 6 different concentrations of samples. These samples represent the amount of metabolites extracted from 10^7, 1.67×10^6, 2.78×10^5, 4.63×10^4, 7.72×10^3, and 1.29×10^3 of cells, respectively. Since each concentration of sample was prepared in triplicate, a total of 18 samples are analyzed in LC-QE-MS.

dx.doi.org/10.1021/ac403845u | Anal. Chem. 2014, 86, 2175−2184

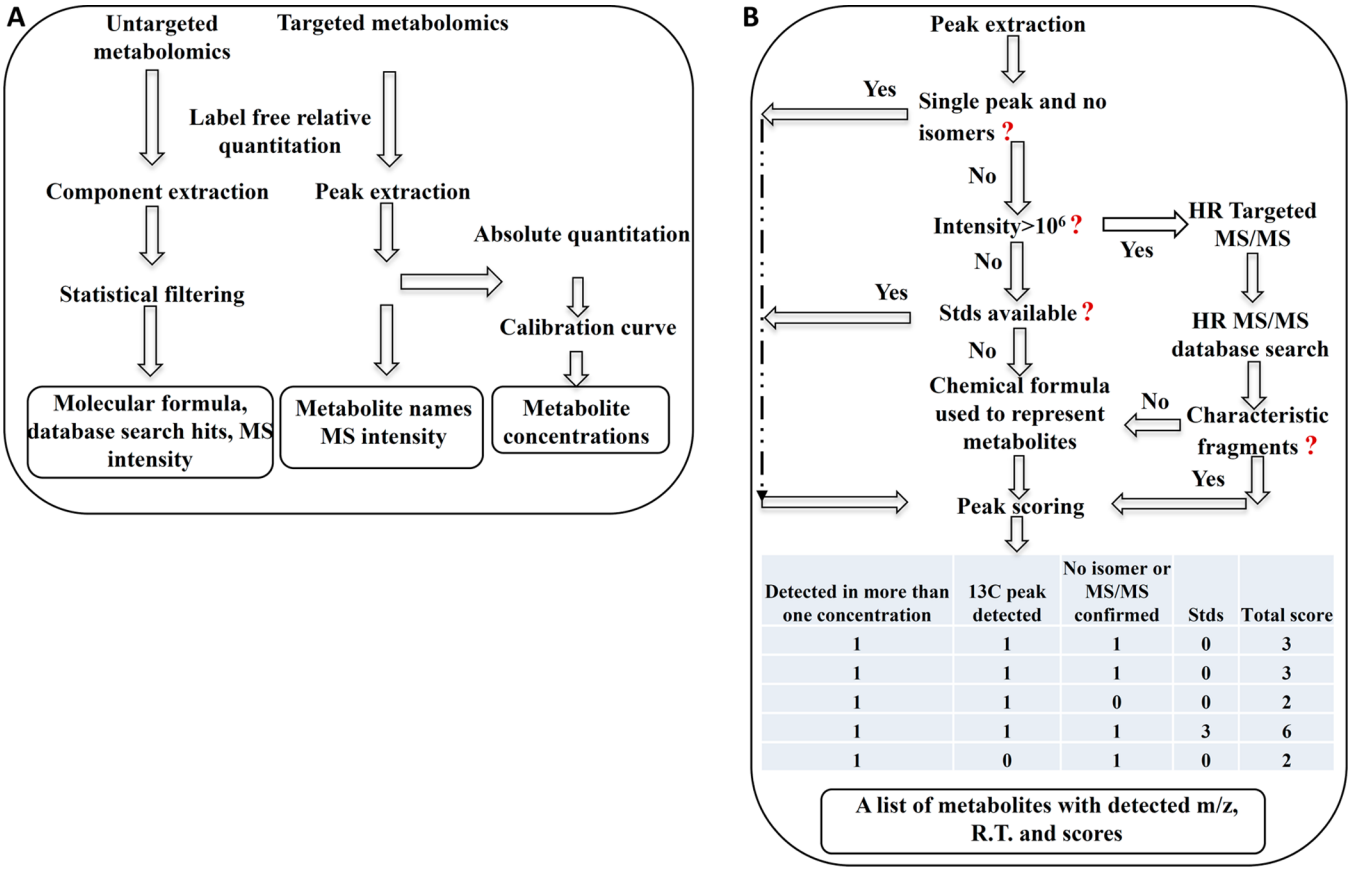

Figure 2. LC-QE-MS data analysis workflow. (A) Workflow for quantitative targeted and untargeted metabolomics study. (B) Workflow for unknown polar metabolites identification and scoring. Abbreviation: Stds = Standards.

Metabolite Extraction from Colorectal Cancer Cell Lines. Eight colorectal cancer cell lines were seeded in 6-well plates at the density of 2×10^5 to 5×10^5 per well for 24 h. Metabolites were extracted as described above, except that 1 mL of extraction solvent was used, instead of 3 mL. Each sample was dissolved into 20 μL of water, and 5 μL was injected to LC-QE-MS. The sequence of sample injections was randomized so that the fluctuation in LC-QE-MS performance was evenly distributed across each sample.

Peak Extraction. Raw data collected from the LC-QE-MS were processed on Thermo Scientific, Sieve 2.0. Peak alignment and detection were performed according to manufacturer protocols. For a targeted metabolomics analysis, a frameseed including 194 metabolites was used for targeted metabolites analysis with data collected in positive mode, while a frame seed of 262 metabolites was used for negative mode, where m/z width is set at 10 ppm. For an untargeted metabolomics analysis, the following parameter values were used to extract untargeted components (pairs of m/z and R.T.): background signal-to-noise ratio, 3; minimum ion count, 1×10^5; minimum scans across the peak, 5; m/z step, 10 ppm.

Statistical Analysis. To assess the linear range, targeted metabolite data was filtered as follows: for each metabolite, if the lowest signal in all of the samples is less than 10^3 and meanwhile the highest signal is less than 10^4, then this metabolite is considered as below the detection limit; if the lowest signal is less than 10^3 but the highest signal is more than 10^4 then replace the low signal with 10^3. Calculations were performed in R computing language (www.r-project.org). The r^2 distribution was represented as a histogram using GraphPad 6.0.

Quantile normalization, unsupervised hierarchical clustering (Pearson, Spearman linkages), and heat map generation were carried out with the software Gene-e (Broad institute, http://www.broadinstitute.org/cancer/software/GENE-E/index.html). The maximum fold change (Maxchange) calculation was carried out in the software package R.

RESULTS

Overview. We first developed a strategy that focuses on measuring polar metabolites (Figure 1, panels A and B). A cold methanol extraction method was used to minimize the perturbation of metabolism in cultured cells.[25,26] LC-HRMS with positive and negative mode switching was employed to expand on the number of metabolites that can be accessed. To achieve high throughput, we considered a chromatography run of 20 min. Both untargeted and targeted metabolomics studies were carried out with the data obtained from the workflow in Figure 1A. Figure 2A describes LC−MS data processing procedures. For the untargeted analysis, neither pre-existing knowledge of metabolites to be measured nor heavy isotope labeled standards (Stds) are required. After a component extraction, the data are further filtered by using multiple criteria, including the coefficient of variation (CV) within replicate samples and the total MS intensity (integrated peak area). Finally, components of interest are selected for a database search based on the detected mass of the selected component with a 10 ppm mass tolerance. For targeted metabolomics, the

dx.doi.org/10.1021/ac403845u | Anal. Chem. 2014, 86, 2175−2184

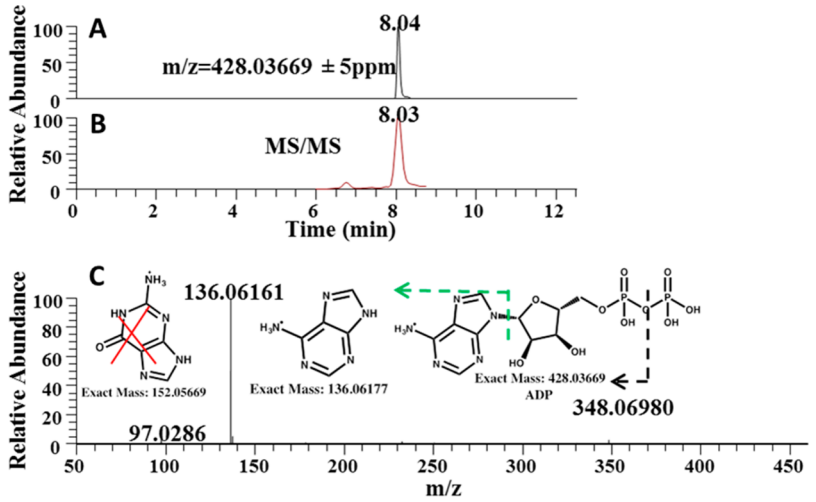

Figure 3. MS/MS of positive ions with m/z of 428.04. (A) The extracted ion chromatogram (EIC) of m/z of 428.03669 (in positive mode) with a mass certainty within 10 ppm. (B) The full MS/MS chromatography of ions with m/z of 428.04 ± 1.25. (C) The MS/MS spectrum. The exact mass of fragment ion is shown below the corresponding fragment ion.

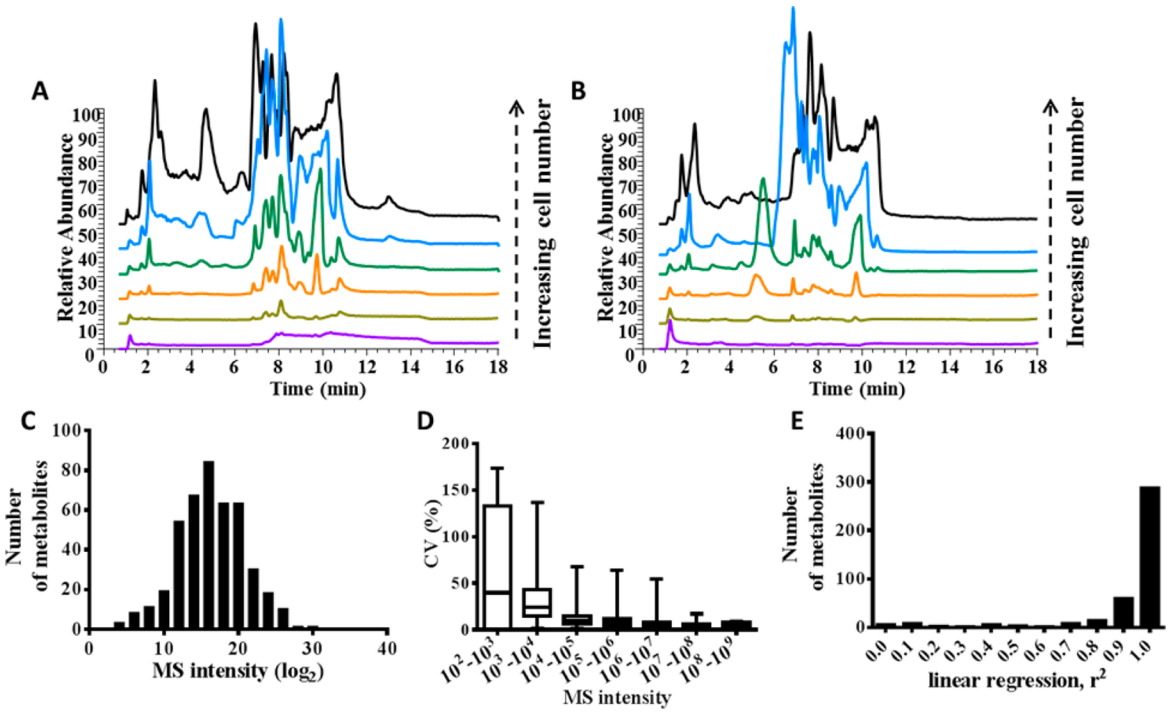

Figure 4. Dynamic range of QE-MS. (A) The total ion chromatogram (TIC) for positive mode for increasing numbers of cells used. (B) TIC for negative mode for increasing numbers of cells used. (C) The $\log_2$-transformed intensity distribution of targeted metabolites in 3×10^5 of HCT8 cells. An average of $n = 3$ biological replicates are considered. (D) The relationship between coefficient of variation (CV) of triplicate samples and MS intensity. The box plot shows the 75th/25th percentile, and the bar represents the median. (E) Linear regression analysis of each metabolite. The number of metabolites with a given r^2 value is shown.

corresponding mass to charge ratio (m/z) and retention time (R.T.) are used for peak extraction.

A comprehensive list of metabolites with theoretical m/z (both in positive and negative mode) was generated based on a recent study.[27] This list was used to generate extracted ion chromatography (EIC) from full scan data. A scoring system was established to evaluate confidence in the metabolite assignments (Figure 2B). A metabolite peak will gain a positive score under any of the following situations: (1) Ions are detected in more than one concentration of sample, (2) a corresponding ^{13}C peak is detected when a labeled extract is used, (3) there exists a unique single peak in the EIC channel and this peak does not contain any known isomers, or if there are known isomers, there are characteristic MS/MS fragments to distinguish the isomers, and (4) authentic standards are injected to confirm the assignment. On the basis of these criteria, we generated a list of 262 metabolites in negative mode and 194 in positive mode, and the following targeted metabolomics data processing was based on this list.

MS/MS Identification of Isomers. An example of an MS/MS-based resolution of isomers is shown in Figure 3. Adenosine diphosphate (ADP) and deoxyguanosine diphos-

dx.doi.org/10.1021/ac403845u | Anal. Chem. 2014, 86, 2175−2184

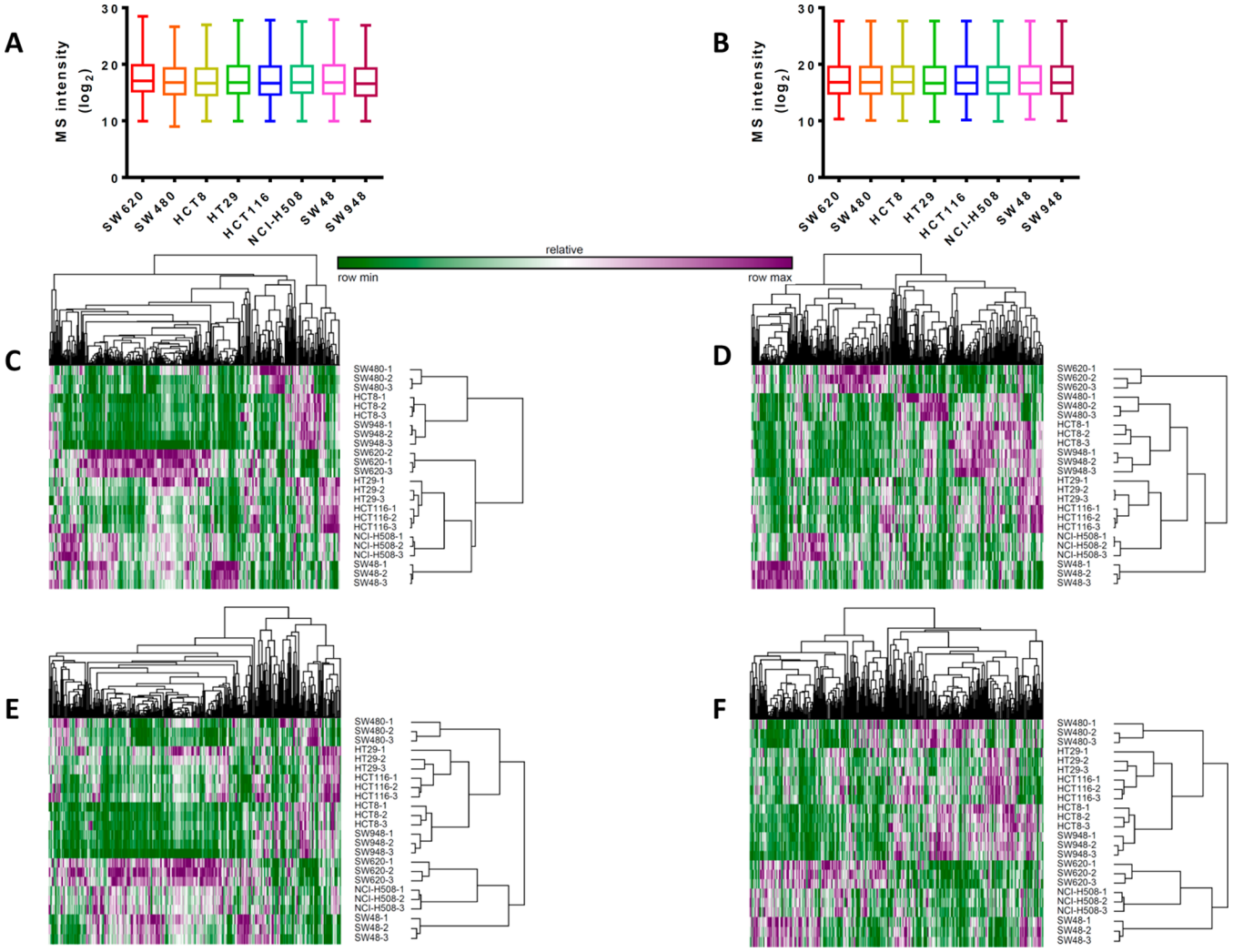

Figure 5. MS intensity distribution and clustering in eight cell lines. (A) MS intensity distributions of cell extracts of colorectal cancer cell lines. Box plots represent the 75th/25th percentile, and the bars represent the median MS intensity. MS intensity is $\log_2$ transformed. (B) MS intensity distribution as in (A) but with quantile normalization. (C) Heat map of Pearson clustering of MS intensity in eight cell lines. (D) Heat map as in (C) but with quantile normalization. (E) Heat map of Spearman ranking clustering of MS intensity in eight cell line. (F) Heat map as in (E) but with quantile normalization. The color code bar is applicable to each of (C–F).

phate (dGDP) are not distinguishable in full scan mode (Figure 3A), since the two molecules have exactly the same elemental composition and, as a result, the same m/z. MS/MS fragmentation by HCD was done at a resolution of 35000. MS/MS peak (Figure 3B) and EIC from full scan (Figure 3A) have the same retention time. At this resolution, MS/MS spectrum has decent intensity and, meanwhile, a very small mass error (1.2 ppm for fragment with m/z = 136.06161), as shown in Figure 3 (panels B and C). In the MS/MS spectrum (Figure 3C), the fragment of m/z = 348.06980 is generated from the cleavage of a phosphate group, which is not characteristic, while the fragment of m/z = 136.06161 is corresponding to adenine, which can only be generated from ADP by cleavage of the ribose group. There is no m/z = 152.05669 (guanine from dGDP) detected, so the peak at 8.03 min is assigned as ADP. We further confirmed this assignment by comparison of ADP and dGDP in a QT of MS/MS spectrum from the Massbank database.[28]

Dynamic Range of Metabolite Quantitation. Having developed a combined metabolomics technology, we next sought to evaluate its quantitative abilities. Metabolites were extracted from 10^7 cells and first diluted 6-fold and then followed by serial dilution resulting in extracts of differing concentrations. The total ion chromatography (TIC) from these 6 concentrations are shown in Figure 4 (panels A and B) (here, the Y axis is normalized by the highest intensity in the sample). Figure 4C demonstrates the MS intensity range across targeted metabolites. Figure 4D demonstrates a strong correlation between CV within triplicate samples and the corresponding MS intensity. As expected, the higher the MS intensity, the lower the measured CV, since a lower signal tends to have more interference from ions with very close m/z values. For metabolites with MS intensities higher than 1×10^6, the CV is within 7.8% (at 75th percentile), while for MS intensities less than 1×10^3, CV varies to a larger extent (132.8% at the 75th percentile). Therefore, we defined an MS intensity of 1×10^3 as the noise level, and in Figure 4E, data are processed further by imputing intensities lower than 1×10^3 with a value of 1×10^3, as described in the methods section. The linear regression of MS intensity (the integrated peak area within the defined retention time window of every m/z) and concentrations is shown in 4E. The TIC increases as the concentration

dx.doi.org/10.1021/ac403845u | Anal. Chem. 2014, 86, 2175–2184

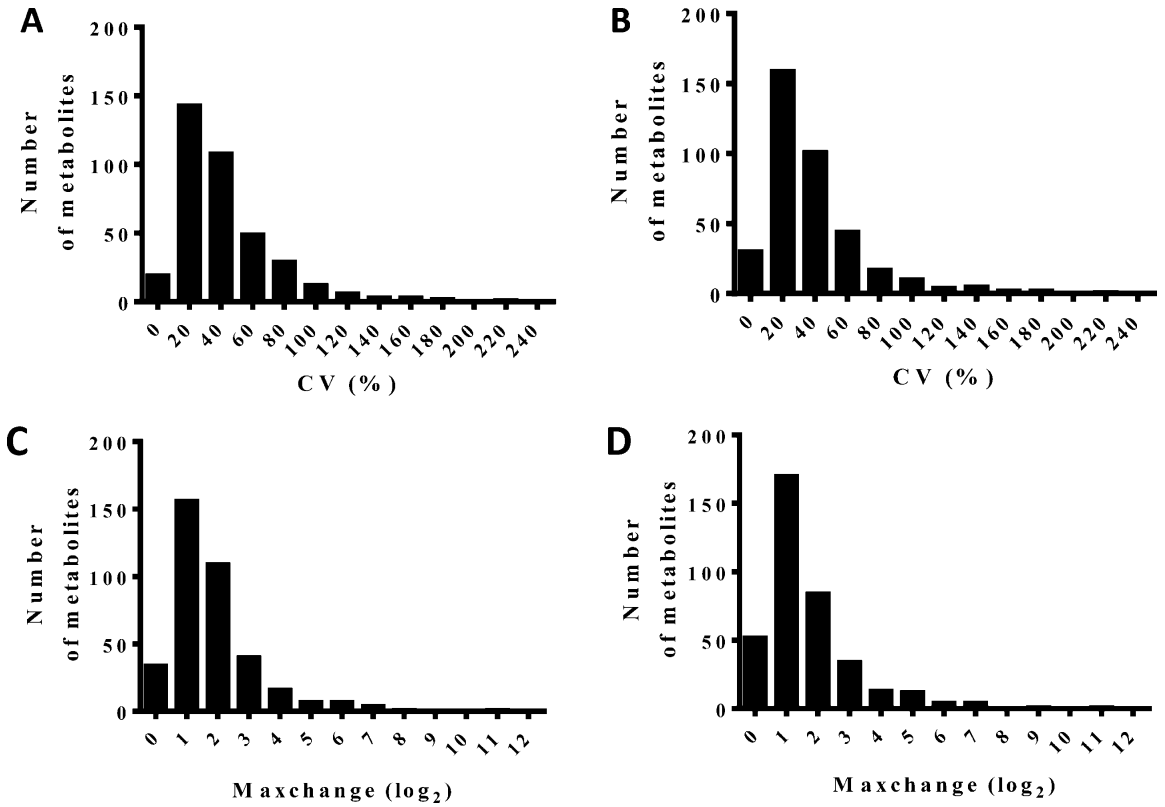

Figure 6. Targeted metabolomic profiling in eight cell lines. (A) CV distribution of metabolites measured in eight cell lines. (B) CV distribution as in (A) except that quantile normalized MS intensity values were used. (C) Maxchange (log_2 transformed) distribution of targeted metabolites. (D) Maxchange distribution as in (C) but with quantile normalized MS intensity values. Abbreviation: Maxchange, the ratio of maximum and minimum MS intensity for every component across cell lines.

of injected metabolites increases, and meanwhile a linear regression analysis of 5 concentrations (excluding the highest saturated concentration) shows that more than 86% of metabolites detected have r^2 values larger than 0.85, implying that over 4 orders of magnitude, the relative mass intensity can accurately reflect metabolite relative levels. The low r^2 in the remaining 14% of metabolites was either because they were not detected at low sample concentration or because they had a poor linear MS response. At a number of 10^7 cells, signals tended to decrease due to strong ion suppression from the biological matrix effect, and also the retention times shift due to overloading of the analyte on the LC column.

Metabolic Profiling of Colorectal Cancer Cell Lines. The method described and discussed in Figures 1 and 2 was then applied to study the metabolite profiles in eight colorectal cancer cell lines: SW620, SW480, HCT8, HT29, HCT116, NCI-H508, SW48, and SW948. A list of 375 measured targeted ions is included in Table 1 of the Supporting Information. Each cell line was cultured in the same medium to avoid confounding effects on metabolism due to differences in nutrient availability. Each cell line was observed to have a different, albeit small, intensity range (Figure 5A), which can be removed with quantile normalization (Figure 5B). An inspection of metabolite intensities was carried out using different clustering algorithms (Figure 5, panels C, D, E, and F). For each representation, the columns represent different metabolites, while the rows represent eight cell lines in triplicate. The effect of quantile normalization becomes apparent when clustering is carried out using linkages corresponding to Pearson correlations. As shown in Figure 5 (panels C and D), SW620, HT29, HCT116, NCI-H508, and SW48 are clustered using raw intensity values, while SW620 is separated from other cell lines when raw intensity is quantile normalized. However, when Spearman correlations are used for the linkages, quantile normalization makes little difference, as expected (Figure 5, panels E and F).

To compare the metabolite profiling variations in different cell lines, the mean values of every three replicates are used to calculate CV and Maxchange (N = 8). Here Maxchange is defined as the ratio of highest to lowest mean intensity observed across the cell line panel. As demonstrated in Figure 6 (panels A and B), 270 out of 375 metabolites have CVs less than 40%, and this number increases to 290 if the quantile normalized values are used. There are 27 out of 375 metabolites with CVs larger than 100% if working with raw values, while this number decreases to 24 if data is quantile normalized. When a Maxchange value is calculated (Figure 6, panels C and D), there are 190 metabolites with Maxchange $\leq$ 2. After quantile normalization, this number increases to 222. For metabolites with Maxchange $\geq$ 32, the number slightly increases from 20 to 22 with quantile normalization.

CV (within triplicates) and MS intensity distributions of untargeted components extracted from the cell line SW620 data based on the parameters listed in the method section are plotted in Figure 7 (panels A and B). The number of components (with MS intensity higher than 10^4) extracted at different cutoff values is plotted in Figure 7C. Here, the 10^4 MS intensity cutoff value is used to avoid working with massive untargeted amounts of components data and to improve data quality. On the basis of Figure 7 (panels B and C), MS intensity

dx.doi.org/10.1021/ac403845u | Anal. Chem. 2014, 86, 2175−2184

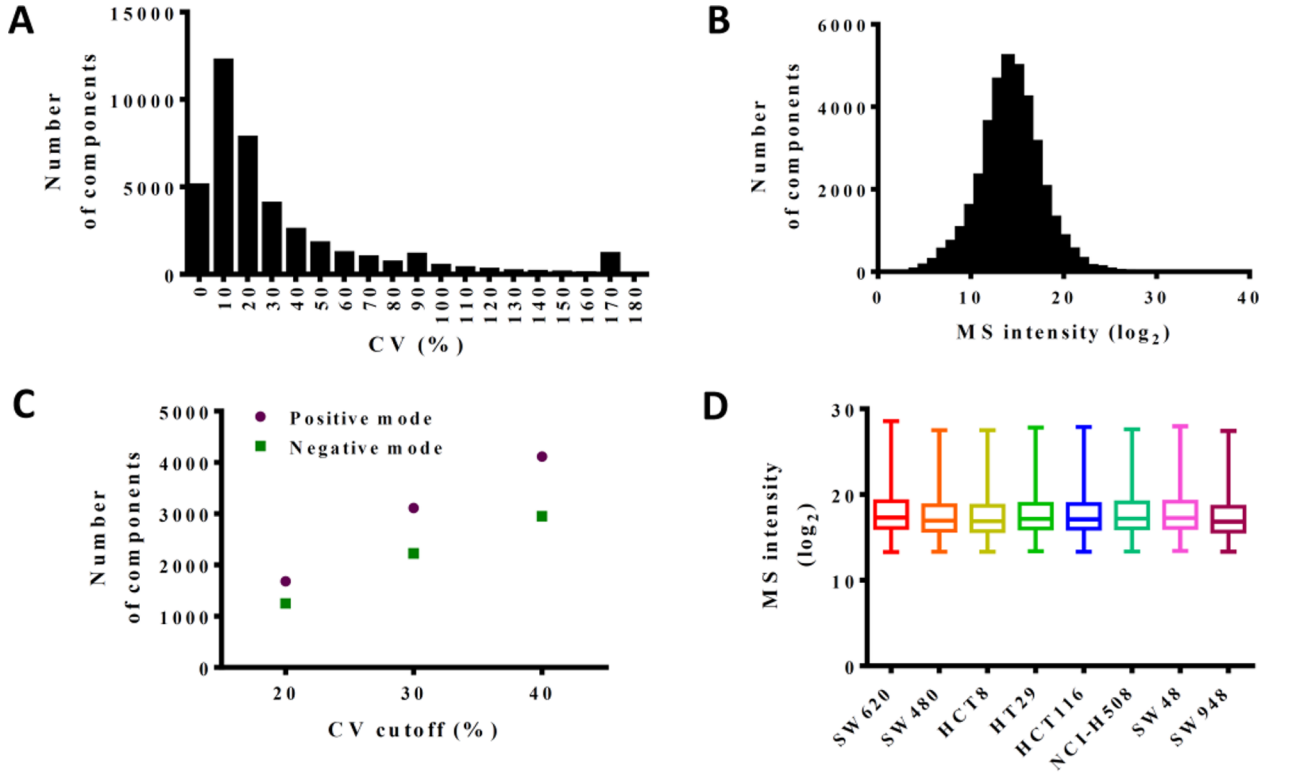

Figure 7. Untargeted component extraction. (A) CV (within biology triplicates) distribution of untargeted components. (B) MS intensity distribution of untargeted components in cell line SW620. (C) The relationship between the number of extracted components and CV cutoff values. (D) MS intensity distributions of cell extract of colorectal cancer cell lines. Box plots represent the 75th/25th percentile, and the bar represents the median. In (A and B), there are no filters applied to the extracted components, while in (D), filters of MS intensity higher than 10^4 and CV (within triplicate) less than 20% were applied.

higher than 104 and CV less than 20% are used to filter the raw intensity data, and the filtered intensity range of each cell line is plotted in Figure 7D. The untargeted components data show similar trends as the targeted metabolite data (Figure 8 (panels A and B). Quantile normalization increases the number of metabolites (Maxchange $\leq$ 2) from 1940 to 2099 and meanwhile decreases the number of metabolites (Maxchange $\geq$ 32) from 34 to 20. When untargeted components intensities are used, as shown in Figure 8 (panels C−F), neither Spearman rank-based clustering nor Pearson correlation-based clustering is affected by quantile normalization of MS intensity. However, compared to the clustering pattern based on the Spearman ranking of 375 targeted metabolites, clustering based on 2931 untargeted components is different for the cell line SW620. The pool of metabolites tends to affect the clustering pattern for both Pearson correlations and Spearman ranking based-clustering. However, there are few conserved subclusters, such as cell lines HT29 and HCT116 and cell lines HCT8 and SW948, which are always clustered together regardless of the clustering method used.

DISCUSSION

Our chromatography method involving HPLC, employed a high pH mobile phase and amide column, coupled with positive/negative switching HRMS enables us to analyze both acidic and basic polar metabolites in a single experiment. Even though this method is not optimized for recovery of any specific metabolite, it nevertheless enables us to cover a large number of polar metabolites and lipids. Moreover, there are some important polar metabolites, such as coenzyme A derivatives and folates, which are not detected in our method. It is either due to their low abundance in the cells lines we used or their instability.[29−31] Therefore, for these metabolites, additional optimization of the extraction procedure will be required.

For a long time, MS was not considered as a quantitative analytical technology, because for metabolites with different chemical structures, they tend to have different ionization efficiency, and even for the same metabolite, if it is measured at different times or spiked into different biological samples, the MS response tends to fluctuate, which is due to the matrix effect.[32,33] Therefore, stable heavy isotope-labeled standards (stds) are commonly spiked into unknown samples to correct the error introduced by sample preparations and MS response fluctuations.[12] In our LC−MS setup, within a wide range, the MS intensity increases in a linear pattern when the corresponding samples are prepared from increasing cell numbers, which gives us high confidence of label-free differential quantitative analysis based on our current workflow. This linearity is observed even when samples of interest are randomly dispersed across large sample runs. Moreover, the CVs within biological triplicates at sufficient peak intensity levels are very small, implying that our current workflow is very reproducible, and subtle biological variations of metabolites in different samples can be measured. However, too much material results in severe ion suppression and also induces overload in the LC, so overall, a smaller number of cells (3×10^5 to 2×10^6 of cells) results in a larger number of metabolites capable of being detected. To overcome the day-to-day variation (i.e., a batch effect), advanced statistic analysis

dx.doi.org/10.1021/ac403845u | Anal. Chem. 2014, 86, 2175−2184

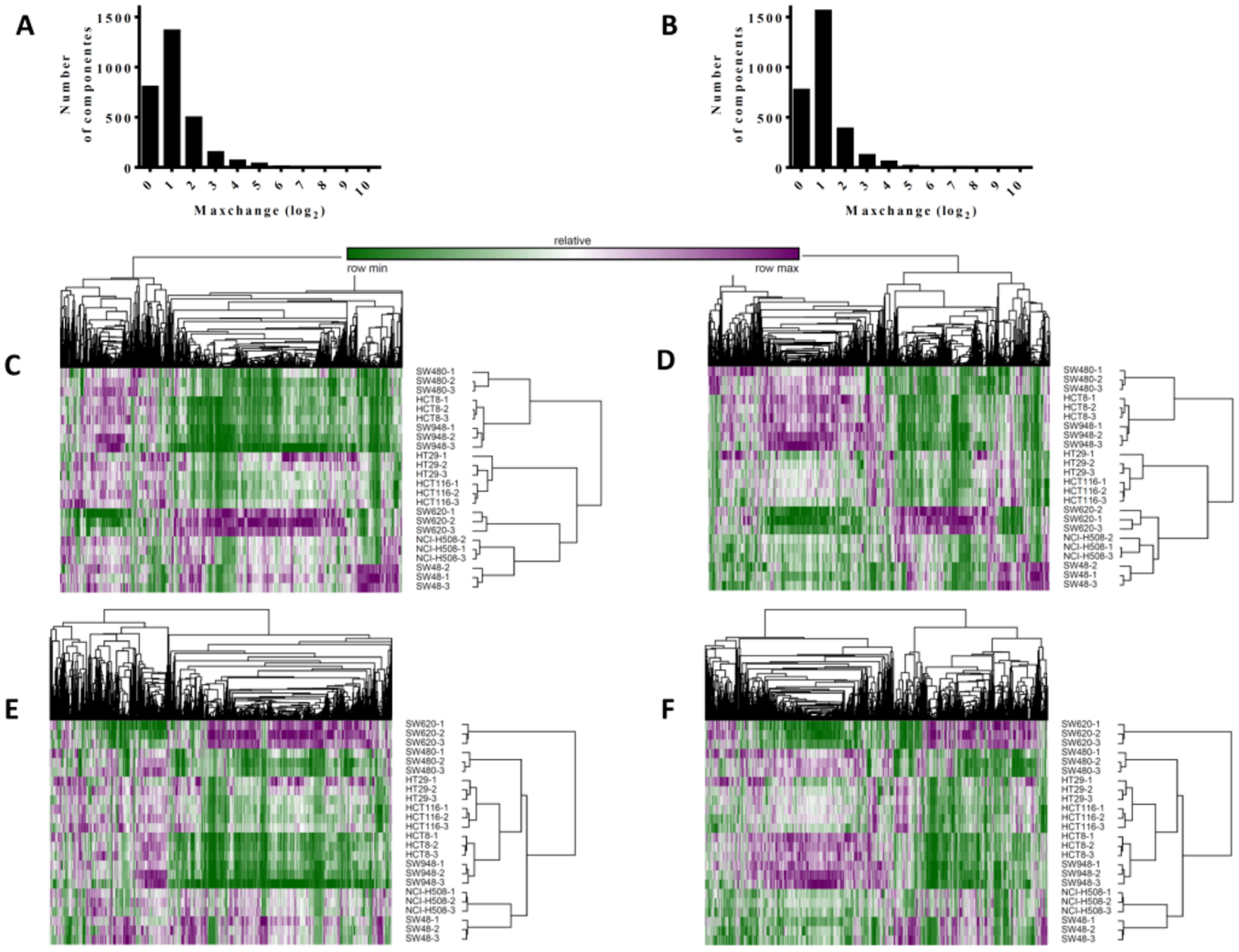

Figure 8. Metabolomic profiling in eight cell lines. (A) Maxchange distribution of cell extract. (B) Maxchange distribution as in (A) except that quantile normalized MS intensity values were used. (C) Heat map of Pearson clustering of MS intensity in eight cell line. (D) Heat map as in (C) but with quantile normalization. (E) Heat map of Spearman ranking clustering of MS intensity in eight cell lines. (F) Heat map as in (E) but with quantile normalization. The color code bar is applicable to (C−F). Abbreviation: Maxchange, the ratio of maximum and minimum MS intensity for every component across cell lines.

might be helpful.[34,35] For absolute quantitation, internal stds or external calibration curves are still required, although it is conceivable that a regression model could circumvent the need for calibration curves in some instances.

In order to compare the metabolomics profiling differences in different cell types, quantile normalization was applied to rescale the metabolite intensities. However, based on our study, quantile normalization results in only modest effects on the CV or Maxchange calculations. Its effect on clustering patterns across the whole data set is however readily apparent.

Since HRMS records almost every ion falling into the scan range and above the limit of detection, little effort is required to build a detection method for each metabolite, but an efficient approach to deal with massive data is critical. Untargeted component-based approaches cover almost every ion recorded in the spectrum if filtering parameters are set at very low values, but this would be inefficient in its computational cost. Practically, a targeted approach is more efficient, even though metabolites outside of the list will be missed. In practice, in order to compare metabolic profiling in different samples, our current targeted list gave a similar cluster pattern as compared to 2931 untargeted components, as shown in Figure 5 (panels C−F) and Figure 8 (C−F). Therefore, in our study, a targeted approach is done first to make metabolic profiling, and then very specific filters are applied to narrow down untargeted components, followed by database searching to make sure no interesting metabolite is missed.

MS/MS data can further increase confidence of unknown metabolite identification, especially for metabolites with isomers and poor separation on LC (Figure 3). However, the MS/MS database is far from complete, and also MS/MS spectra in the database were generated from different types of mass spectrometry with different fragmentation methods. It has been shown that the MS/MS pattern is dependent on how collision energy is applied and also the elemental composition of the collision gas.[28] Moreover, to obtain useful MS/MS spectra, a precursor ion of sufficient intensity is required. Due to these limitations, efforts are needed to further develop a high throughput method for MS/MS data processing and metabolite identification.

Eight colorectal cancer cell lines show three distinct metabolic patterns which gives us a hint that the metabolic

dx.doi.org/10.1021/ac403845u | Anal. Chem. 2014, 86, 2175−2184

enzymes are either differentially expressed or with variant activities across these cell lines. This potentially suggests opportunities for biomarker analysis in metabolomics applications.

CONCLUSION

The platform demonstrated here is applicable for targeted and untargeted label-free polar metabolites quantitative analysis. Besides cell culture work, this method is being applied to biomarker studies using tissues, serum, and other human fluids, and provides a resource to the metabolomics field. With such a technology, further investigation that connects metabolite profile to biological phenotype is possible.

ASSOCIATED CONTENT

Supporting Information

The authors declare no conflicts of interest. This material is available free of charge via the Internet at http://pubs.acs.org.

AUTHOR INFORMATION

Corresponding Author

*E-mail: Locasale@cornell.edu.

Notes

The authors declare no competing financial interest.

ACKNOWLEDGMENTS

The authors would like to acknowledge Detlef Schumann and Jennifer Sutton (Thermo Scientific) for valuable discussions on data processing. The authors would also like to thank Brandon Barker, Tamar Melman. and Mahya Mehrmohamadi (Cornell University) for help with data analysis. Research reported in this publication was supported by the National Cancer Institute of the National Institutes of Health under Award Number R00CA168997. The content is solely the responsibility of the authors and does not necessarily represent the official views of the National Institutes of Health.

REFERENCES

(1) Denkert, C.; Budczies, J.; Kind, T.; Weichert, W.; Tablack, P.; Sehouli, J.; Niesporek, S.; Konsgen, D.; Dietel, M.; Fiehn, O. *Cancer Res.* **2006**, *66*, 10795−10804.

(2) Smith, C. A.; Want, E. J.; O'Maille, G.; Abagyan, R.; Siuzdak, G. *Anal. Chem.* **2006**, *78*, 779−787.

(3) Cornett, D. S.; Reyzer, M. L.; Chaurand, P.; Caprioli, R. M. *Nat. Methods* **2007**, *4*, 828−833.

(4) Sreekumar, A.; Poisson, L. M.; Rajendiran, T. M.; Khan, A. P.; Cao, Q.; Yu, J.; Laxman, B.; Mehra, R.; Lonigro, R. J.; Li, Y.; Nyati, M. K.; Ahsan, A.; Kalyana-Sundaram, S.; Han, B.; Cao, X.; Byun, J.; Omenn, G. S.; Ghosh, D.; Pennathur, S.; Alexander, D. C.; Berger, A.; Shuster, J. R.; Wei, J. T.; Varambally, S.; Beecher, C.; Chinnaiyan, A. M. *Nature* **2009**, *457*, 910−914.

(5) Griffin, J. L.; Shockcor, J. P. *Nat. Rev. Cancer* **2004**, *4*, 551−561.

(6) Christofk, H. R.; Vander Heiden, M. G.; Harris, M. H.; Ramanathan, A.; Gerszten, R. E.; Wei, R.; Fleming, M. D.; Schreiber, S. L.; Cantley, L. C. *Nature* **2008**, *452*, 230−233.

(7) Dang, L.; White, D. W.; Gross, S.; Bennett, B. D.; Bittinger, M. A.; Driggers, E. M.; Fantin, V. R.; Jang, H. G.; Jin, S.; Keenan, M. C.; Marks, K. M.; Prins, R. M.; Ward, P. S.; Yen, K. E.; Liau, L. M.; Rabinowitz, J. D.; Cantley, L. C.; Thompson, C. B.; Vander Heiden, M. G.; Su, S. M. *Nature* **2009**, *462*, 739−744.

(8) Vander Heiden, M. G.; Locasale, J. W.; Swanson, K. D.; Sharfi, H.; Heffron, G. J.; Amador-Noguez, D.; Christofk, H. R.; Wagner, G.; Rabinowitz, J. D.; Asara, J. M.; Cantley, L. C. *Science* **2010**, *329*, 1492−1499.

(9) Locasale, J. W.; Grassian, A. R.; Melman, T.; Lyssiotis, C. A.; Mattaini, K. R.; Bass, A. J.; Heffron, G.; Metallo, C. M.; Muranen, T.; Sharfi, H.; Sasaki, A. T.; Anastasiou, D.; Mullarky, E.; Vokes, N. I.; Sasaki, M.; Beroukhim, R.; Stephanopoulos, G.; Ligon, A. H.; Meyerson, M.; Richardson, A. L.; Chin, L.; Wagner, G.; Asara, J. M.; Brugge, J. S.; Cantley, L. C.; Vander Heiden, M. G. *Nat. Genet.* **2011**, *43*, 869−874.

(10) Locasale, J. W.; Melman, T.; Song, S.; Yang, X.; Swanson, K. D.; Cantley, L. C.; Wong, E. T.; Asara, J. M. *Mol. Cell. Proteomics* **2012**, *11*, M111 014688.

(11) Scherb, J.; Kreissl, J.; Haupt, S.; Schieberle, P. *J. Agric. Food Chem.* **2009**, *57*, 9091−9096.

(12) Ciccimaro, E.; Blair, I. A. *Bioanalysis* **2010**, *2*, 311−341.

(13) Southam, A. D.; Payne, T. G.; Cooper, H. J.; Arvanitis, T. N.; Viant, M. R. *Anal. Chem.* **2007**, *79*, 4595−4602.

(14) Dettmer, K.; Aronov, P. A.; Hammock, B. D. *Mass Spectrom. Rev.* **2007**, *26*, 51−78.

(15) Lu, W.; Clasquin, M. F.; Melamud, E.; Amador-Noguez, D.; Caudy, A. A.; Rabinowitz, J. D. *Anal. Chem.* **2010**, *82*, 3212−3221.

(16) Michalski, A.; Damoc, E.; Hauschild, J. P.; Lange, O.; Wieghaus, A.; Makarov, A.; Nagaraj, N.; Cox, J.; Mann, M.; Horning, S. *Mol. Cell. Proteomics* **2011**, *10*, M111 011015.

(17) Fedorova, G.; Randak, T.; Lindberg, R. H.; Grabic, R. *Rapid Commun. Mass Spectrom.* **2013**, *27*, 1751−1762.

(18) Blasco, H.; Corcia, P.; Pradat, P. F.; Bocca, C.; Gordon, P. H.; Veyrat-Durebex, C.; Mavel, S.; Nadal-Desbarats, L.; Moreau, C.; Devos, D.; Andres, C. R.; Emond, P. *J. Proteome Res.* **2013**, *12*, 3746−3754.

(19) Li, T. M.; Chen, J.; Li, X.; Ding, X. J.; Wu, Y.; Zhao, L. F.; Chen, S.; Lei, X.; Dong, M. Q. *Anal. Chem.* **2013**, *85*, 9281−9287.

(20) Concheiro, M.; Lee, D.; Lendoiro, E.; Huestis, M. A. *J. Chromatogr., A* **2013**, *1297*, 123−130.

(21) Nagaraj, N.; Kulak, N. A.; Cox, J.; Neuhauser, N.; Mayr, K.; Hoerning, O.; Vorm, O.; Mann, M. *Mol. Cell. Proteomics* **2012**, *11*, M111 013722.

(22) Kelstrup, C. D.; Young, C.; Lavallee, R.; Nielsen, M. L.; Olsen, J. V. *J. Proteome Res.* **2012**, *11*, 3487−3497.

(23) Gallien, S.; Duriez, E.; Crone, C.; Kellmann, M.; Moehring, T.; Domon, B. *Mol. Cell. Proteomics* **2012**, *11*, 1709−1723.

(24) Poulsen, J. W.; Madsen, C. T.; Young, C.; Kelstrup, C. D.; Grell, H. C.; Henriksen, P.; Juhl-Jensen, L.; Nielsen, M. L. *J. Proteomics* **2012**, *75*, 3886−3897.

(25) Yuan, M.; Breitkopf, S. B.; Yang, X.; Asara, J. M. *Nat. Protoc.* **2012**, *7*, 872−881.

(26) Shyh-Chang, N.; Locasale, J. W.; Lyssiotis, C. A.; Zheng, Y.; Teo, R. Y.; Ratanasirintrawoot, S.; Zhang, J.; Onder, T.; Unternaehrer, J. J.; Zhu, H.; Asara, J. M.; Daley, G. Q.; Cantley, L. C. *Science* **2013**, *339*, 222−226.

(27) Thiele, I.; Swainston, N.; Fleming, R. M.; Hoppe, A.; Sahoo, S.; Aurich, M. K.; Haraldsdottir, H.; Mo, M. L.; Rolfsson, O.; Stobbe, M. D.; Thorleifsson, S. G.; Agren, R.; Bolling, C.; Bordel, S.; Chavali, A. K.; Dobson, P.; Dunn, W. B.; Endler, L.; Hala, D.; Hucka, M.; Hull, D.; Jameson, D.; Jamshidi, N.; Jonsson, J. J.; Juty, N.; Keating, S.; Nookaew, I.; Le Novere, N.; Malys, N.; Mazein, A.; Papin, J. A.; Price, N. D.; Selkov, E., Sr.; Sigurdsson, M. I.; Simeonidis, E.; Sonnenschein, N.; Smallbone, K.; Sorokin, A.; van Beek, J. H.; Weichart, D.; Goryanin, I.; Nielsen, J.; Westerhoff, H. V.; Kell, D. B.; Mendes, P.; Palsson, B. O. *Nat. Biotechnol.* **2013**, *31*, 419−425.

(28) Horai, H.; Arita, M.; Kanaya, S.; Nihei, Y.; Ikeda, T.; Suwa, K.; Ojima, Y.; Tanaka, K.; Tanaka, S.; Aoshima, K.; Oda, Y.; Kakazu, Y.; Kusano, M.; Tohge, T.; Matsuda, F.; Sawada, Y.; Hirai, M. Y.; Nakanishi, H.; Ikeda, K.; Akimoto, N.; Maoka, T.; Takahashi, H.; Ara, T.; Sakurai, N.; Suzuki, H.; Shibata, D.; Neumann, S.; Iida, T.; Tanaka, K.; Funatsu, K.; Matsuura, F.; Soga, T.; Taguchi, R.; Saito, K.; Nishioka, T. *J. Mass Spectrom.* **2010**, *45*, 703−714.

(29) Ishikawa, M.; Fujino, T.; Sakashita, H.; Morikawa, K.; Yamamoto, T. *Tohoku J. Exp. Med.* **1995**, *175*, 55−67.

(30) Garbis, S. D.; Melse-Boonstra, A.; West, C. E.; van Breemen, R. B. *Anal. Chem.* **2001**, *73*, 5358−5364.

(31) Pfeiffer, C. M.; Fazili, Z.; McCoy, L.; Zhang, M.; Gunter, E. W. *Clin. Chem.* **2004**, *50*, 423−432.
(32) Annesley, T. M. *Clin. Chem.* **2003**, *49*, 1041−1044.
(33) Taylor, P. J. *Clin. Biochem.* **2005**, *38*, 328−334.
(34) De Livera, A. M.; Dias, D. A.; De Souza, D.; Rupasinghe, T.; Pyke, J.; Tull, D.; Roessner, U.; McConville, M.; Speed, T. P. *Anal. Chem.* **2012**, *84*, 10768−10776.
(35) De Livera, A. M.; Olshansky, M.; Speed, T. P. *Methods Mol. Biol.* **2013**, *1055*, 291−307.